

Pontificia Universidad Católica del Perú



**SHAKE TABLE TEST SERVICES FOR GETTY
SEISMIC ADOBE PROJECT AND PROJECT
TERRA**

AGREEMENT NUMBER 0600031872

FINAL REPORT

DANIEL E. TORREALVA

APRIL 2005

SHAKE TABLE TEST SERVICES FOR GETTY SEISMIC ADOBE PROJECT AND PROJECT TERRA

FINAL REPORT – APRIL 2005

CONTENTS

- 1.0 Introduction
- 2.0 Project description
- 3.0 Description of test specimens.
- 4.0 Preliminary tests and masonry properties.
- 5.0 Instrumentation of models and testing procedure.
- 6.0 Seismic behavior of models.
- 6.1 Model 1.
- 6.2 Model 2.
- 7.0 Experimental results.
- 7.1 Maximum displacement values.
- 7.2 Maximum acceleration values.
- 7.3 Time histories:
- 8.0 Comparison with previous seismic simulation tests.
- 8.1 Pseudo P- δ curves.
- 9.0 Conclusions and recommendations.

SHAKE TABLE TEST SERVICES FOR GETTY SEISMIC ADOBE PROJECT AND PROJECT TERRA

AGREEMENT NUMBER 0600031872

FINAL REPORT – FEBRUARY 2005

1.0 Introduction

Existing earthen buildings are about half of the housing inventory in the world. In many places where these buildings are located, strong earthquakes are also very frequent, causing every time considerable material damage and irreparable loss of lives and cultural property. In spite of its seismic vulnerability, vernacular earthen houses, however, are still being used by millions of people in many countries because of cultural, climatic and economic reasons.

In the last 30 years, several research projects have attempted to solve the problem of the low seismic resistance of vernacular earthen buildings. They have addressed both, the new and the existing buildings made of adobe using natural (wood and cane) and industrial materials (steel bars, steel mesh and cement). In both cases, the most effective solution found so far, is to provide the building with a continuous reinforcement, horizontal and vertical elements placed at a certain distance ranging from 0.50 to 1.0 meters or the use of a steel mesh with or without cement mortar plaster.

For new buildings, and is to incorporate an internal mesh of vertical whole canes every 50 cm and horizontal split canes every 3 or 4 layers firmly tied at the corners and wall intersections and at the crown wooden beam (Vargas 1978, Torrealva 1985, Ottazzi et al. 1988, Bariola et al. 1988).

For existing buildings two solutions have proven to be effective: completely reinforce the building with an external welded wire mesh anchored to the foundation and top beam (Scawthorn 1985) and partially reinforce the buildings with an external steel mesh covering both sides and tying them through the adobe walls (Zegarra et al. 1997, CERESIS 1999), this solution would require a sand cement mortar plaster for the sake of protection of the steel mesh. Both solutions can also be applied to new buildings.

There are however some inconveniences in the use of these solutions, first, it implies materials, wire mesh and cement that are much too expensive for their use in vernacular housing, second, the sand cement plaster have the inconvenience of incompatible

stiffness with the adobe walls, and third, for buildings of cultural value, a sand cement stucco on an adobe wall, will change its plastic appearance.

In the search for widely available and compatible materials, the structural polymer mesh (geogrid) appears as a promising solution for reinforcing new and existing earthen buildings without changing its appearance and providing adequate seismic resistance. With this aim, the Getty Conservation Institute and the Catholic University of Peru agree to carry out this initial research project.

2.0 Project description

The main objective of the project was to prove that external compatible mesh reinforcement can be used to guarantee the survival of an earthen building during strong earthquakes. The project consisted on the testing of two 3 x 3 meter reinforced mud brick models to seismic simulation tests using a shaking table, since these dynamic tests are the best way to understand the seismic behavior of earthen buildings (Krawinkler 1978). Two types of external and compatible mesh were used, the first one with natural materials using cane and vegetal rope and the second one with an industrial polymer geogrid.

3.0 Description of test specimens.

The two test specimens had the same configuration and overall dimensions shown in Figure 1a and 1b. They consisted of four walls 3,21 m long, variable height, and 0,26 m thick, The North and South walls are identical and include a central window opening, making a symmetric structure in the direction subjected to the seismic loading. The two seismically transverse walls were different, the East wall with a door opening and the West wall without any opening and bigger height. Each specimen was built over a reinforced concrete foundation ring beam, which also served to anchor the specimen to the shaking table and as support during the transportation of the wall from the construction yard to the laboratory. A wooden crown beam was placed on top of each specimen to transmit the gravity loading corresponding to a typical dwelling roof.

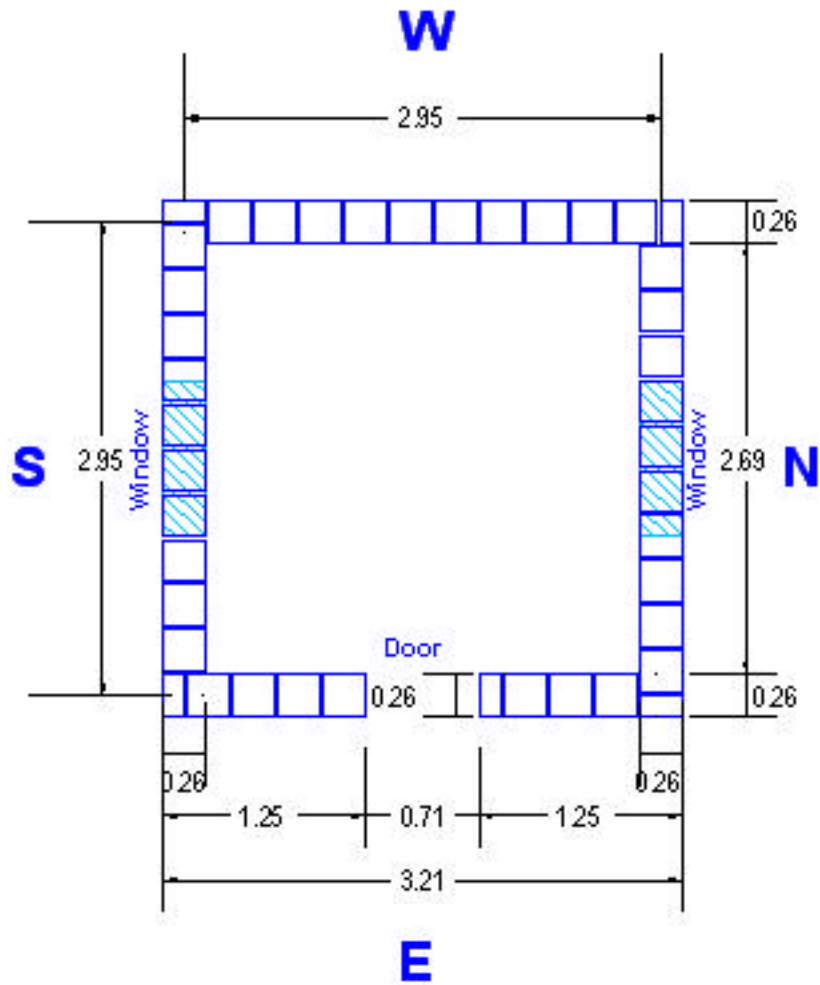


Figure 1a. Plan view and adobe block layout

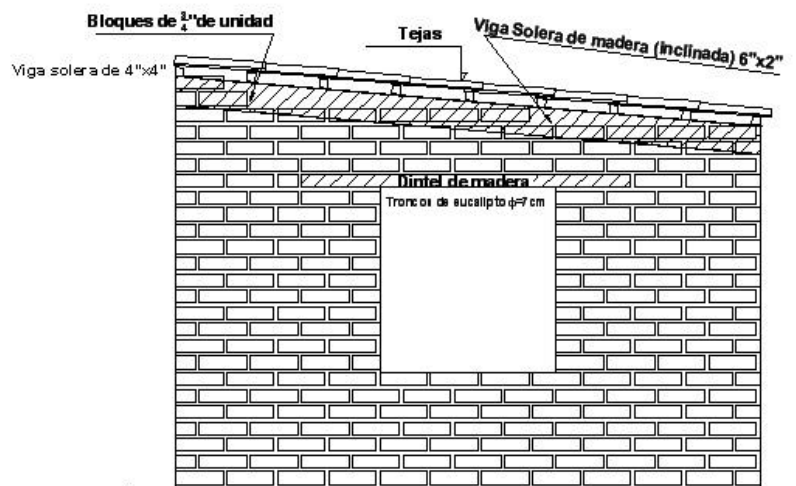


Figure 1b. South wall elevation

Both models were built using traditional techniques, representative of traditional, seismically vulnerable adobe construction in Peru. The adobe blocks are joined with

mud mortar, see figure 2. The blocks used were 0,07 x 0,26 x 0,26 m. and were fabricated with soil, coarse sand and straw in proportion 5:1:1 the layout pattern for the adobe blocks was the same for the two models. A wooden joist roof with cement tiles were used on both specimens. The total weight of each specimen was around ??? kN.



Figure 3. Typical construction process

Model 1 was externally reinforced with a natural mesh composed of natural cane as vertical elements and “cabuya” rope as horizontal elements on both sides of the wall. The canes and cabuya rope were connected through the wall with a small diameter yute thread (see figure 4).



Figure 4. Cabuya rope for horizontal reinforcement and yute thread.



Figure 5a. Placing the vertical reinforcement in small trenches previously cut in the wall.

The deep of the trenches is about 1 cm in order to maintain the strength of the wall.

Figure 5b. After placing the vertical canes on both sides of the wall, they are tied with horizontal cabuya rope, to form the structural grid. The joints of the grid are connected through the wall with yute thread.



Figure 5c. Two holes are perforated at both sides of the vertical cane, so the yute thread holds the cane and the rope tightly



Figure 6. Model 1 reinforced with natural materials and plastered on one side.

Model 2 was externally reinforced with an industrial material, in this case polymer geogrid TENSAR BX 1200 was used as external reinforcement. The mesh was placed on both sides of the wall by pieces and connected through the wall with plastic strings every 25 cm horizontal and vertically spaced (see figure 7 to 14).



Figure 7. Drilling holes in the wall, spaced every 30 cm.



Figure 8. The geogrid comes in rolls of 3 by 50 meters. From it, it's cut in the necessary dimensions with a pair of scissors.

Figure 9. Portions of geogrid are placed on the walls in a continuous way and stretched as much as possible. Specially at the corners.



Figure 10. The mesh is provisionally fixed in position by nailing it to the wall.



Figure 11. After placing the mesh completely, it is sowed through the wall in order to connect it with the mesh at the opposite side. A long needle and plastic thread is used for this purpose.

Figure 12. View of the plastic thread before tying. The overlapping of the mesh can also be appreciated.



Figure 13. Tying the thread for confinement of the adobe wall with the geogrid.



Figure 14. Model 2, reinforced with polymer geogrid and plastered for one side.

In both models, plaster on the surface was placed on half of the model in order to appreciate the behavior of the model with and without plaster.

4.0 Preliminary tests and masonry properties.

Five axial compression tests on prisms and three diagonal compression tests on wallets were performed to establish the mechanical properties of the adobe masonry (figures 15a and 15b). The piles were constructed with five adobe blocks, with overall dimensions of 25 x 25 x 43 cm, the vertical deformation was measured in order to calculate the Elasticity Modulus. The wallets had dimensions of 25 x 50 x 50 cm. The average compression strength for the piles was 0.87 Mpa (8.7 kg/cm²) and the average Elasticity Modulus was 482 Mpa (4,320 kg/cm²). From the diagonal compression tests, the average shear strength was 0.068 Mpa (0.68 kg/cm²). The results of the tests are shown in tables 1 and 2.



Figure 15a. Diagonal compression test.



Figure 15b. Axial compression test.

PILE	f'_m (MPa)	E_m (MPa)
Pile-1	0.83	653
Pile-2	0.98	319
Pile-3	0.82	462
Pile-4	0.83	310
Pile-5	0.80	417
Stand. Dev. σ	0.07	139
Average	0.85	432
Aver - σ	0.78	293

Table 1. Compressive strength and Elasticity Modulus of adobe piles.

WALLETE	v'_m (MPa)
Wall -1	0.070
Wall-2	0.085
Wall-3	0.048
Stand. Dev. σ	0.019
Average	0.068
Average - σ	0.049

Table 2. Shear strength of adobe walls from diagonal compression tests.

5.0 Instrumentation of models and testing procedure.

The models were instrumented with six accelerometers and eight displacement transducers as shown in figure 16. Acceleration and displacement were measured at the top of each wall and the mid height of West Wall, only displacements were measured below the windows on the North and South walls. Table displacement and acceleration and pressure on the hydraulic actuator were also measured

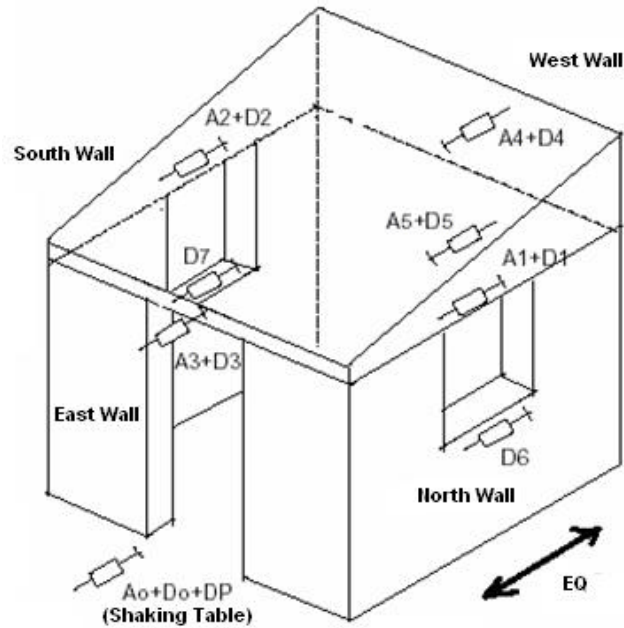


Figure16. Instrument configuration.

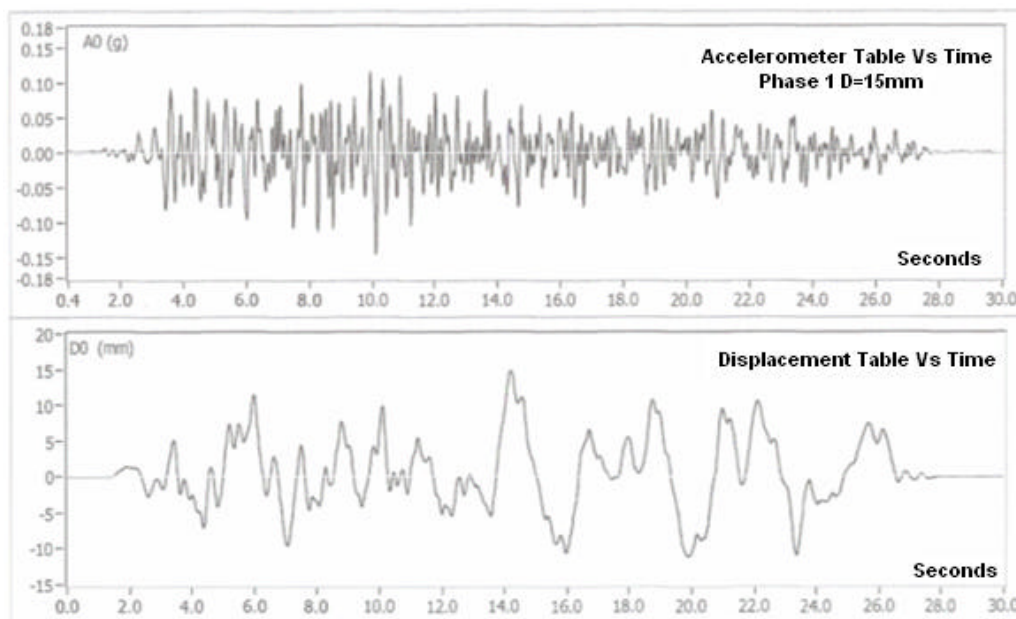


Figure 17. Acceleration and displacement time history of table motion.

Both models were subjected to several motions of increasing intensity, the signal was derived from a record of the Peruvian earthquake of May 31st, 1970, see figure 17.

Model 1 was subjected to six motions with peak acceleration of 0.15g, 0.30g, 0.60g, 0.80g and two motions of 1.0g. It was tested on Tuesday January 18th, 2005.

Model 2 was subjected to seven motions with peak acceleration of 0.15g, 0.30g, 0.60g, 0.80g, 1.0g and two motions of 1.2g. It was tested on Thursday January 20th, 2005

6.0 Seismic behavior of models.

Description and visual observation made during testing are presented in this section.

6.1 Model 1.

Model 1 behaved elastically until phase 3 with peak acceleration of 0.6g, in phase 4, a vertical crack, all the way from top to bottom, caused the separation of the west wall. However, the wall was kept in place by the horizontal rope reinforcement. Phases 5 and 6, both with 1g peak acceleration shake the model causing partial loss of the stucco and extensive cracking, dividing the wall into small pieces, partial and total collapse was avoided by the natural external mesh. It was clear that the seismic energy was dissipated by big horizontal displacements of transverse walls.



Figure 18. Model 1 after testing, view of north wall.

After removing the plaster from the north wall, it was clear that the south wall suffered more damage than the north wall. The different type of connection of the lintel with the ring beam (diagonal wooden strips), caused a hammering action against the upper portion of the wall. Also the plaster in the north wall increased the stiffness and strength in that wall. See figures 7 and 8.



Figure 19. Model 1 South wall, without plaster. Damage is widespread but greater at the lintel level

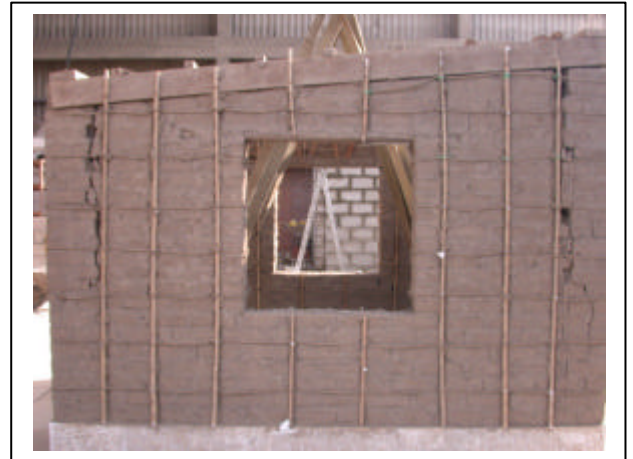


Figure 20. Model 1 North wall, plastered side. Vertical cracks appear at the intersection with transversal walls.

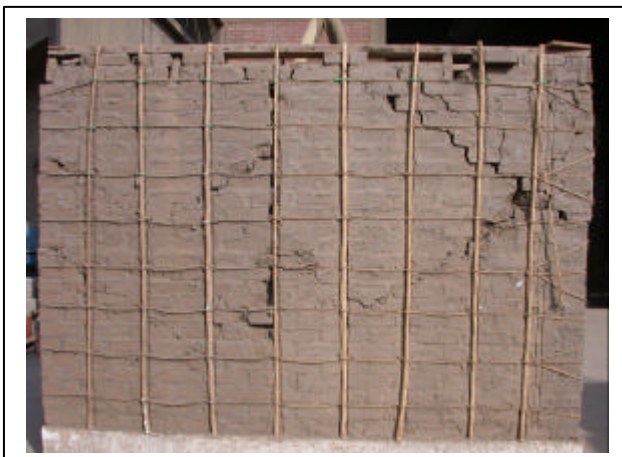


Figure 21. Model 1 West wall, The right half without plaster show greater damage than the left half.



Figure 22. Model 1 East wall, The left side without plaster. Show greater damage than the right side

6.2 Model 2.

Model 2 also remained in the elastic range until phase 3, in phase 4, small cracks appeared in the walls, the cracks were more visible in the plastered side since is difficult to observe them in the side with the mesh exposed. In phase 5 the model slide from its base almost as a rigid body, without having significant damage. Phases 6 and 7, both with 1.2g of peak acceleration caused additional cracking in the walls and also sliding in the base (figure 22). After the test, only small cracking was visible in the north wall, been more significant in the south wall. See figure 23.



Figure 23. Sliding of the base in the North wall.



Figure 24. Model 2 after removing the plaster and the polymer mesh. The East and North wall shown here present only small cracking.

After removing the external mesh from the walls, it could be appreciated that the plastered side (North Wall) suffered less damage than the South Wall. In the case of the plastered side, the polymer mesh acted as if it were an internal reinforcement inside the stucco and the stucco adhered to the wall, so, as it has been proved in a previous research, the internal reinforcement increases the initial shear strength of the wall.



Figure 25. Model 2 North Wall without plaster. The wall is completely cracked after the test with more extensive damage in the left hand pier.



Figure 26 Model 2 South Wall, plastered side. The wall shows only small cracking with one vertical crack at the left wall intersection. See the sliding of the base at the right lower corner.



Figure 27. Model 2 West Wall. The right hand side without plaster shows cracking at mid height. The left plastered side shows damage at the lower part because the sliding of the North Wall.



Figure 28. Model 2 East Wall. Only small cracking appear on this wall. The sliding can be seen at the lower left corner and a vertical crack in the right side.

7.0 Experimental results.

Extensive data in the form of digital signals was obtained from the displacement and acceleration transducers, eight displacement transducers and six accelerometers gave time histories in five runs for model 1 and six runs for model 2, making a total of 154 time histories. Processing and interpretation of this data is a major task, and only the most significant data has been processed in this report, further data analysis can be performed as future work of graduate and undergraduate students.

7.1 Maximum relative displacements.

Tables 3 and 4 show the peak relative displacement obtained in each instrument and each phase for model 1 and 2 respectively.

In model 1, there is a complete information for phases 1 to 4. In phase 5 the instruments D1 and D6 in the north wall did not record the displacements because a loosen part of stucco hit the connection threads, for this reason, in phase 6 all the displacement transducers were removed in prevention of a partial collapse, that did not occur. Is worth mention that phases 5 and 6 had the same peak table displacement of 120 mm.

In model 2 all the instrumentation was kept until the last phase with the exception of LVDT's D6 and D7, since the behavior of the model was such, that not partial collapse was expected. The instrument distribution is shown in figure 29.

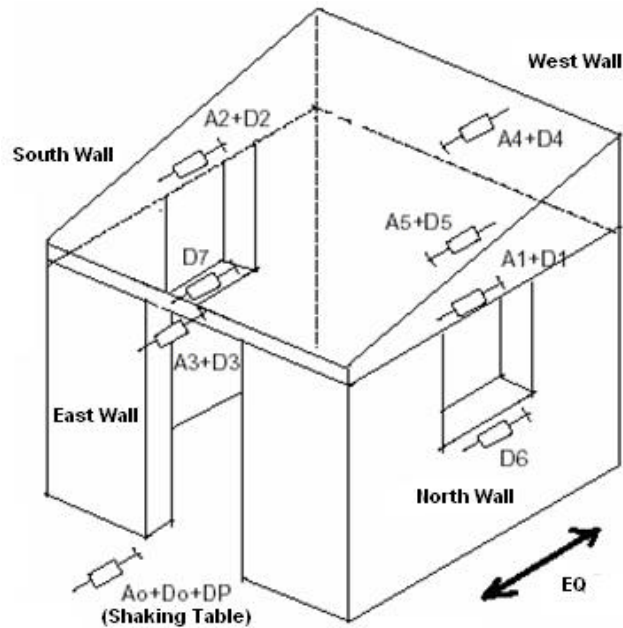


Figure 29. Instrument configuration.

The instrumental results are in agreement with the observed behavior, until phase 3 both models behaved elastically.

In phase 4 the west wall in model 1 suffered vertical cracks along the intersection with walls north and south, after these cracks opened, the west wall underwent big displacements, vibrating almost independently from the rest of the model, the displacements at the top and the middle of that wall was 122.27 mm and 62.80 mm respectively. In comparison to model 1, the displacements in model 2 in the same locations were almost 4 times smaller 30.93 mm for the top and 17.78 mm for the middle.

In phase 5, the displacements D1 and D6 of the north wall were not recorded properly for model 1, but the type of behavior was similar to phase 4, with the west wall having the bigger displacements, 212.89 mm for the top and 106.11 mm for the middle, the displacements for model 2 in the same locations were 73.51 mm and 40.78 mm respectively.

In phases 6 and 7, only model 2 had instrumentation, showing bigger displacements than phase 5. The displacement D6, shows big values of relative displacement because the sliding of the north wall relative to the base.

One important fact that was appreciated in the test and is corroborated with the instrumental information is the difference in behavior of the north (D1) and south (D2) walls. The north wall was covered with stucco in both models whereas the south wall was left with the reinforcement exposed. The top displacements of these walls show less displacement in the plastered wall than in the wall without plaster, in phase 4 for model 1, the displacement D1 is 5 times less than the displacement D2. In model 2 for phases 4 and 5 the displacement D1 is also 5 times less than the displacement D2. For phases 5 and 6 this difference is not shown in the table because of the sliding of the north wall.

Since the model is symmetrical in the direction of motion, it is expected that similar earthquake forces are applied to north and south wall, therefore this results show that the plaster over the external reinforcement increase substantially the stiffness of the wall.

Relative Displacements (mm) Model 1						
LVDT	Phase1	Phase 2	Phase 3	Phase4	Phase5	Phase6
D1	0.60	0.87	4.22	12.30	*****	-
D2	1.16	1.01	7.39	66.12	95.76	-
D3	0.74	2.04	7.64	40.51	128.57	-
D4	0.40	1.36	6.40	122.27	212.89	-
D5	0.48	1.07	4.17	62.80	106.11	-
D6	0.50	0.95	1.64	2.07	*****	-
D7	0.45	0.70	1.81	3.61	10.76	-

Table 3. Peak relative displacements for Model 1.

Relative Displacements (mm) Model 2							
LVDT	Phase1	Phase 2	Phase 3	Phase4	Phase5	Phase6	Phase7
D1	0.61	1.28	2.77	7.63	18.25	81.01	73.01
D2	0.54	1.22	3.40	37.35	90.96	117.01	142.77
D3	0.66	1.42	4.29	30.46	58.39	100.52	118.42
D4	0.39	1.23	5.34	30.93	73.51	112.18	119.50
D5	0.61	1.19	2.85	17.78	40.78	63.90	-
D6	0.74	1.40	2.66	2.65	9.07	63.22	-
D7	0.50	0.70	1.40	7.23	18.40	34.75	-

Table 4. Peak relative displacements for Model 2.

7.2 Maximum acceleration values.

Tables 5 and 6 show the peak values of acceleration for each instrument and each phase for models 1 and 2.

All the instruments in phase 6 for model 1 were removed from the model in prevention of partial collapse.

In both models the maximum accelerations were recorded at the top of the east wall and with this data the and the peak table acceleration, the Dynamic Amplification Factor (DAF) was computed. Model 1 shows an increasing DAF with the increase of table motion whereas model 1 shows a decay in the value of DAF after phase 4 as can be seen in figure 30.

The decay in model 2 can be explained by the sliding of the model that dissipated energy by friction at the base, in a similar way to the base isolated buildings.

Instrument	Model 1					
	Phase 1	Phase 2	Phase 3	Phase 4	Phase 5	Phase 6
A0	0.139	0.305	0.606	0.772	0.907	-
A1	0.152	0.000	0.670	0.984	1.328	-
A2	0.152	0.365	0.760	1.153	1.054	-
A3	0.213	0.535	1.312	2.352	3.669	-
A4	0.168	0.433	0.859	1.732	1.812	-
A5	0.139	0.360	0.671	0.914	1.217	-
amáx	0.213	0.535	1.312	2.352	3.669	-
DAF	1.534	1.751	2.166	3.047	4.046	-

Table 5. Peak accelerations in Model 1.

Instrument	Model 2						
	Phase 1	Phase 2	Phase 3	Phase 4	Phase 5	Phase 6	Phase 7
A0	0.139	0.304	0.604	0.831	0.898	1.055	1.051
A1	0.131	0.321	0.637	0.804	1.026	0.915	0.874
A2	0.153	0.356	0.710	1.064	1.540	1.139	1.104
A3	0.178	0.463	0.974	2.263	1.601	2.246	2.257
A4	0.165	0.418	0.806	1.360	1.829	2.000	1.730
A5	0.137	0.345	0.661	0.839	1.041	1.042	0.824
amáx	0.178	0.463	0.974	2.263	1.829	2.246	2.257
DAF	1.286	1.525	1.613	2.724	2.037	2.130	2.147

Table 6. Peak accelerations in Model 2.

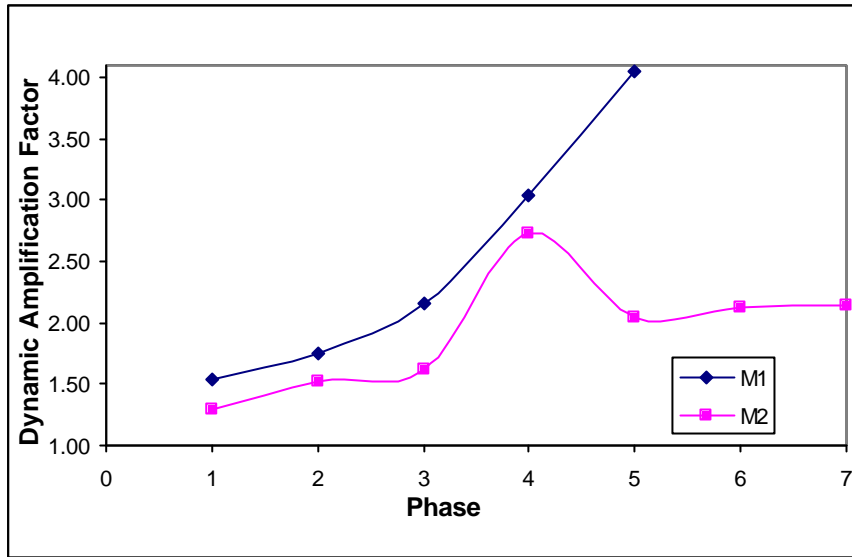


Figure 30. Dynamic Amplification Factor for models 1 and 2.

7.3 Time histories.

Acceleration and relative displacements time histories were recorded in most of the phases at given points shown in figure 29. All time histories recorded are contained in a digital file annex to this report. The relevant information from top displacements in phase 4, Model 1 and phase 6, Model 2 are described in this section.

In phase 4 of Model 1, the peak base displacement was 80 mm and the peak table acceleration 0.8g approximately, in this phase, the model start cracking at several points, mainly at both corners of west wall isolating it and producing vibrations with big amplitude, as a result of this, the time history of D4 shows bigger displacements than the rest of the roof (the maximum is 122 mm). On the contrary, the minimum displacement, ten times less, are found in the north wall (D2, maximum of 12 mm), this wall was plastered with mud and showed less cracking than the rest of the model. The south wall (without plaster) and the east wall (the door wall) showed similar time histories with 66 and 40 mm of maximum displacement respectively. In both cases the time histories show a permanent deformation which may be caused by the cracking of the walls near the point of measure. See figure 31.

Phase 6 in Model 2 had a peak base displacement of 120mm and a peak base acceleration of 1.2g approximately. In this phase, the north wall (D1) at about 11 seconds of motion slide in the base a distance of 40 mm approximately having after that a minimum amplitude vibration. The south wall however (D2), vibrated with the maximum top displacements during all test, being clear, the torsional motion with a rigidity center near the north wall. The south wall ended with a small permanent deformation produced by the extensive inner cracking. The west and east walls showed similar behavior, with big amplitude vibration and permanent deformations produced also by the inner cracking. See figure 32.

From the top displacement time histories, is clear that, even with reinforcement, the four walls vibrate independently from one another, the lightweight roof is far away of behaving as a rigid diaphragm. In both models, the north wall (plastered) was more rigid than the south wall, creating torsional effects.

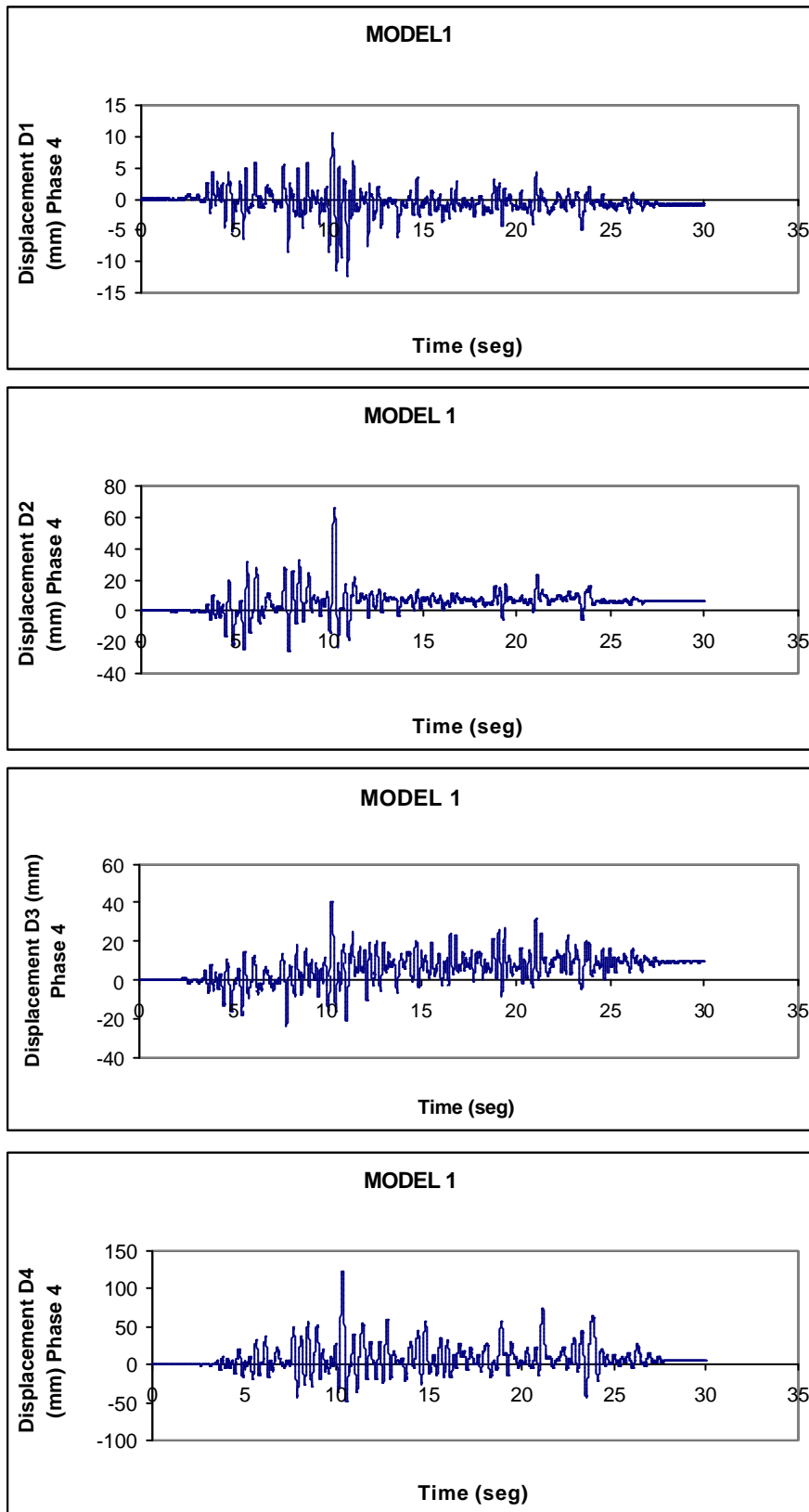


Figure 31. Displacements at top of Model 1 for phase 4.

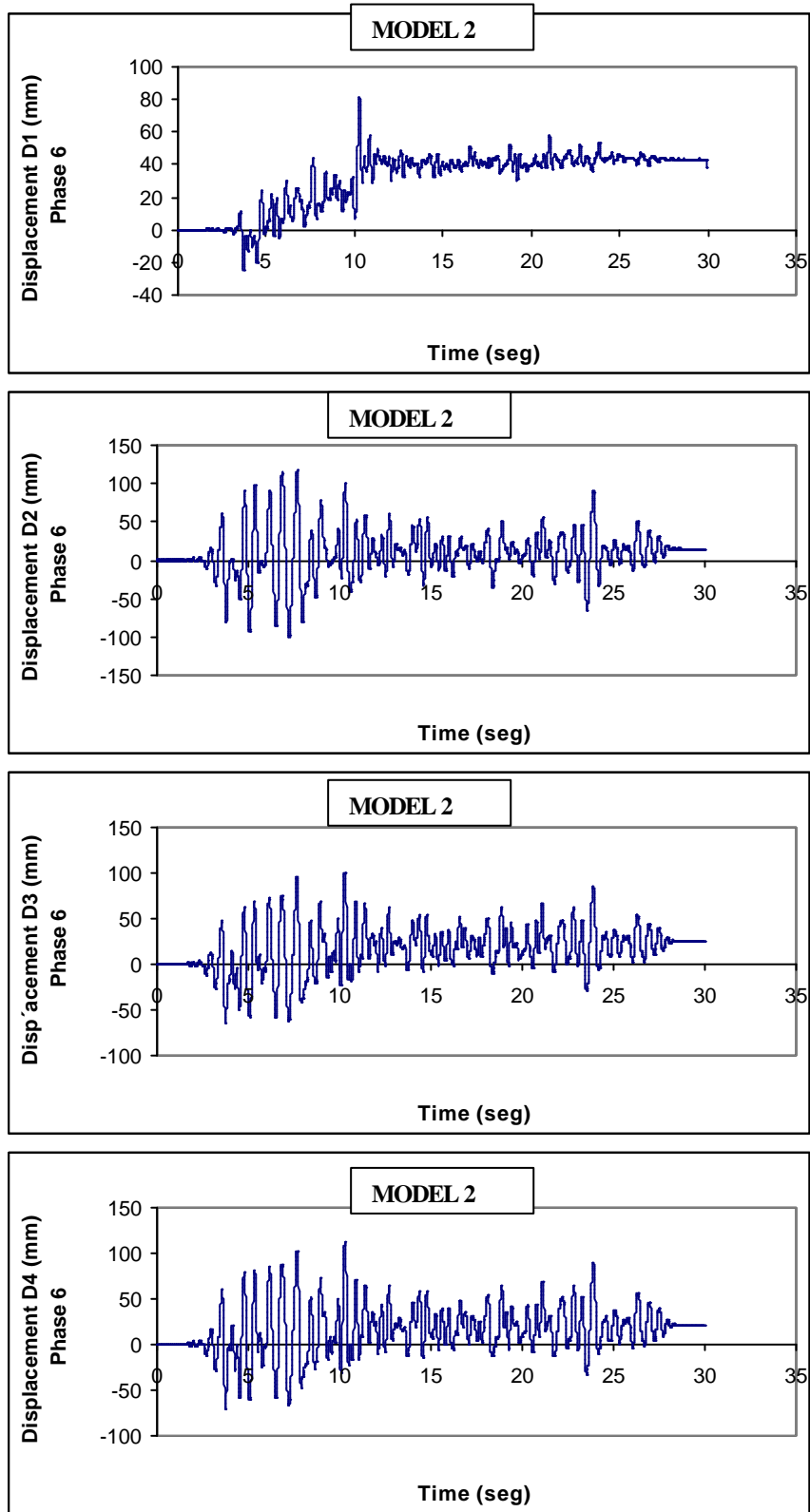


Figure 32. Displacements at top of Model 2 for phase 6.

8.0 Comparison with previous seismic simulation tests.

One of the objectives of the project was to compare the effectiveness of the external compatible mesh with other similar tests carried out at the Structures Laboratory in the year 2001. Models 1 and 2 of this project were built with the same dimensions, and subjected to equal seismic motions in order to make a comparison. Also, most of the instruments were placed in the same locations, so, time histories can be compared.

Three similar models were built and tested seismically in the year 2001, a brief description of reinforcement in each model follows:

M1B was plain adobe model without any kind of reinforcement, and served as baseline.

M2B Was partially reinforced at the corners and around the top with a welded wire mesh covered with a sand cement mortar.

M3B had the same reinforcement than M2B, plus a reinforced concrete ring beam at the lintel level.

All the models and their final state after testing are shown in table 7.

From table 7 we can infer that partial reinforcement of welded wire mesh, when plastered with sand cement mortar ends in a brittle failure with partial collapses. The big difference in stiffness between the adobe wall and the cement mortar layer, makes this last one being the only one to carry the horizontal forces until it reaches a brittle failure. Scawthorn (1988) reported that seismic simulation test of adobe models completely reinforced with welded wire mesh on both sides but without any plaster stood motions with several g of peak acceleration.

The polymer and natural meshes are more compatible materials with the adobe wall, and combined with a mud plaster work jointly during all phases of motion, controlling the cracking of the walls for small and medium intensity motions and preventing the collapse for strong intensity motions.






Model	Characteristics	Ultimate Behavior	Final State
M1	Exterior natural mesh, vertical cane and horizontal “cabuya” rope	Phases 5 and 6, both with p.g.a.=1.0-g: Vertical cracks at every corner, Crushing of the south wall near the lintel. Extensive cracking by the mortar joints in the east and west walls but remaining stable.	
M2	Exterior industrial polymer geogrid mesh.	Phases 6 and 7 both with p.g.a.=1.2-g: Vertical cracks in every corner, moderate overall cracking, 7 cm sliding of the base at the north wall, remains in stable equilibrium.	
M1B	Unreinforced	Phase 4 (p.g.a= 0.8g): Extensive cracking appear in every wall, vertical cracking at the corners. Phase 5 (p.g.a.=1.0-g): Partial collapse of south-east corner, remaining in unstable equilibrium.	
M2B	Partial exterior mesh of welded wire plus sand cement mortar	Phase 6 (p.g.a.=1.2-g): Collapse of south wall including the lintel., 15 cm sliding at the base, extensive cracking in the non plastered portions of the wall. The final state is unstable.	
M3B	Partial exterior welded wire mesh with sand cement palster plus reinforced concrete ring beam and concrete dowels at the corners.	Phase 6 (p.g.a.=1.2-g): Shear failure at the lintel level, collapse of non plastered walls, 10 cm sliding at the base. The final state is unstable.	

Table 6. Comparison of five models with different types of reinforcement.

8.1 Pseudo P-d curves.

Since there is not a uniform displacement at the top of model, and every wall has a different time history displacement, independent curves has been plotted for the maximum displacement in every phase, in the horizontal axis and the maximum shear base of the same phase in the vertical axis. In this way we get a pseudo Force-Displacement curve that depicts the behavior of that particular wall during the whole test. Therefore, every phase of test can be considered as an incremental value of the force related to the displacement obtained.

Figures 33 to 36 compare this pseudo P- δ curves for all models and for each wall. From these curves we can say that M2 and M3B models have the maximum shear strength (about 12,000 kg) and both increase almost three times the strength of the unreinforced model. (4,000 kg). Models M1 and M2B have also similar strength and both increase twice the strength of the unreinforced model.

In general, it can be said that the models with external mesh undergone greater deformations, being this fact notorious in the transversal west wall. For the in plane action, the M2 north wall had the maximum lateral deformation after cracking due to the sliding of the base.

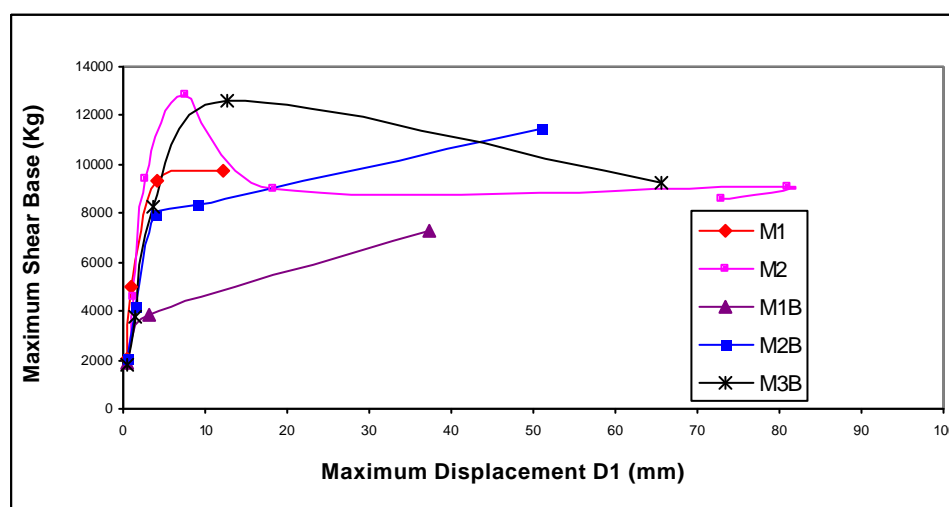


Figure 33. Pseudo P-d curves for the north wall.

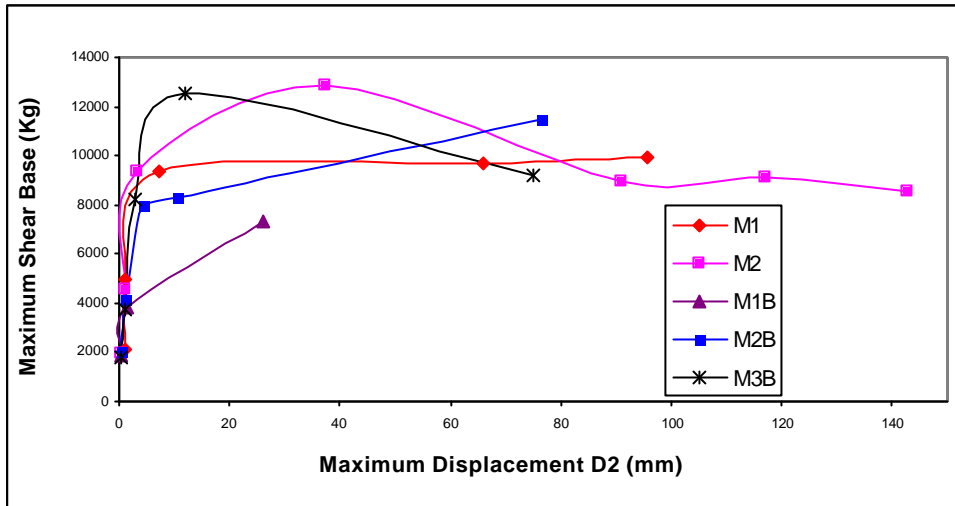


Figure 34. Pseudo P-d curves for the south wall.

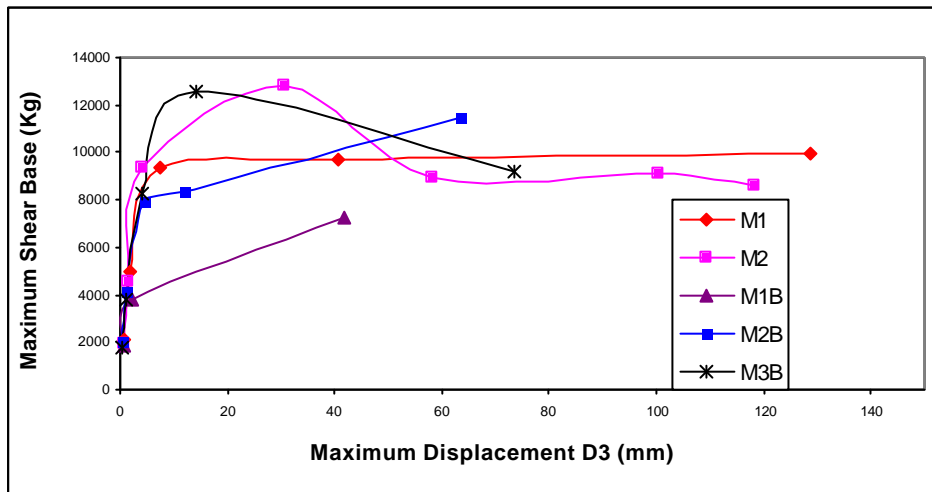


Figure 35. Pseudo P-d curves for the east wall.

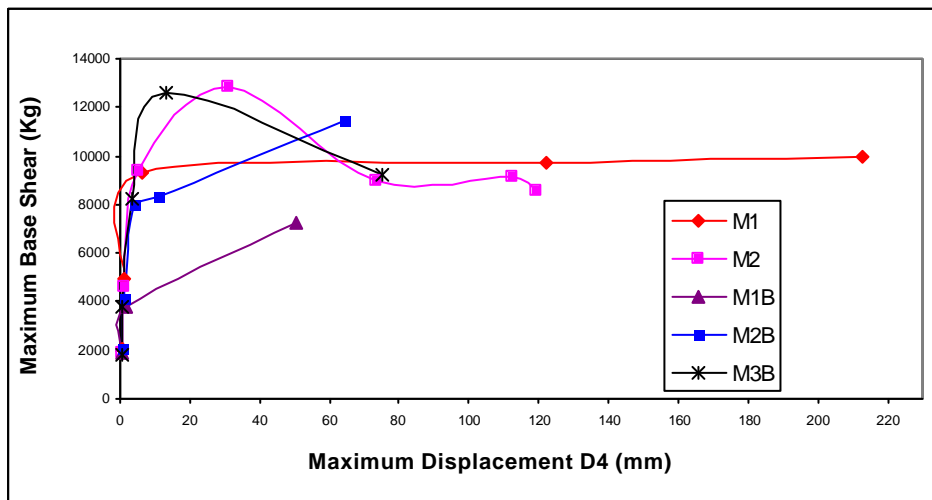


Figure 36. Pseudo P-d curves for the west wall.

9.0 Conclusions and recommendations.

Placing an external, natural or industrial mesh on both sides and connected through the thickness of the adobe wall is an effective way to avoid partial or total collapse of adobe buildings even for severe earthquakes.

If the mesh is not covered with mud stucco, the initial strength is the same as the plain unreinforced wall and the mesh starts working after the wall is cracked. The mesh confines afterwards, the different pieces in which the wall is broken avoiding partial or total collapses.

The mud plaster over the mesh greatly increases the initial shear strength and the stiffness of the wall. By controlling the lateral displacements, it prevents the cracking of the wall in great extent. This is particularly notorious in Model 2.

Based on the results, Model 2 can be considered as the upper limit of the amount of external reinforcement, because the wall is completely covered with the mesh and the mesh is an industrial material with appropriate stiffness and strength.

Model 1 on the contrary, can be considered as near the lower limit of the external reinforcement, because of the natural material used and the vertical and horizontal spacing between reinforcements.

Further testing should aim at rationalizing the amount of polymer mesh used as reinforcement. Between the many options, external vertical and horizontal strips of mesh and internal horizontal mesh strips combined with external vertical mesh strips can also be an effective means of getting an earthquake resistant solution for earthen buildings.

Similar dynamic testing on models, can be used to corroborate the appropriateness of this solution to different architectural typologies of earthen buildings in the world.

9.0 List of references

Scawthorn C. "Strengthening of Low-Strength Masonry Buildings: Analytical and Shaking Table Test Results". Dames and Moore San Francisco California. Research Supported by the National Science Foundation USA, 1985.

Torrealva D. "A Field and laboratory Tested Technique for Retrofitting Adobe Houses in Seismic Areas". Middle east and Mediterranean Regional Conference on Earthen and Low-Strength Masonry Buildings in Seismic Areas. Ankara, Turkey, 1986

Bariola J, Vargas J, Torrealva D, Ottazzi G. 1988. "Earthquake Resistant Provisions for Adobe Construction in Peru". 9th World Conference on Earthquake Engineering. Tokyo-Kyoto, Japan.

Blondet M, Ginocchio F, Marsh C, Ottazzi G, Villa García G, Yep J. 1988. "Shaking Table Test of Improved Adobe Masonry Houses". 9th World Conference on Earthquake Engineering. Tokyo-Kyoto, Japan.

Blondet M, Madueño I, Torrealva D, Villa García G, Ginocchio F. 2004. "Reinforced of Adobe Constructions with Industrial Elements" Earthbuild2005 New Zeland.

Vargas, J. 1978. Recommendations for Design and Constructions of Adobe Houses. Experimental Study. In Spanish. International Symposium 4 February 1976 Earthquake, and the Reconstructions Process. Guatemala.

Zegarra L, Quiun D, San Bartolomé A, Giesecke A. 1997. Reinforcement of Existing Adobe Dwellings 2nd part: Seismic Test of Modules. In Spanish. XI National Congress of civil Engineer. Trujillo, Peru.

Zegarra L, Quiun D, San Bartolomé A, Giesecke A. 2001. Behavior of Reinforced Adobe Dwellings in Moquegua, Tacna and Arica during the 23-06-2001 Earthquake. In Spanish. XIII National Congress of civil Engineer. Puno, Peru.

Lima, April 2005.